# Field-driven oscillation and rotation of a multiskyrmion cluster in a nanodisk

Yan Liu, Huan Yan, Min Jia, Haifeng Du, An Du, and Jiadong Zang

Phys. Rev. B **95**, 134442 — Published 26 April 2017

DOI: 10.1103/PhysRevB.95.134442

# Field-driven oscillation and rotation of multi-skyrmion cluster in a nanodisk

Yan Liu[1], Huan Yan[1], Min Jia[1], Haifeng Du[2,3], An Du[1], Jiadong Zang[4]

[1]College of Sciences, Northeastern University, Shenyang, Liaoning Province 110819, China

[2]High Magnetic Field Laboratory, Chinese Academy of Science (CAS), Hefei, Anhui Province 230031, China

[3]Collaborative Innovation Center of Advanced Microstructures, Nanjing University, Jiangsu Province 210093, China

[4]Department of Physics and Materials Science Program, University of New Hampshire, Durham, NH 03824, USA

## Abstract

The field-driven magnetization dynamics of multi-skyrmion cluster in nanodisks is investigated by micromagnetic simulation and analytical calculation. Under a weak in-plane static magnetic field, the multi-skyrmion cluster shows an oscillatory motion around an equilibrium position, which resembles the dynamical behavior of the conventional torsional pendulum. We show that this oscillation is induced by a restoring torque acting on the skyrmion generated by the potential energy determined by the angle of the skyrmion orientation. Moreover, the multi-skyrmion cluster can be driven to rotate by an in-plane rotating magnetic field. The rotation directions and frequencies are fully determined by the number of the skyrmions.

## Introduction

A simple harmonic oscillator, such as spring oscillator, pendulum, and torsional pendulum, arises when the particle is subjected into a confining potential. Its damping towards the equilibrium position is captured by the inertia of particles. In fact, this concept is applicable to not only physical particles, but also spin textures such as magnetic domain walls, whose oscillation was observed and mass was measured [1-2].

Besides the conventional domain wall, magnetic skyrmion is a topologically stable spin texture with particle-like properties. This topologically stable spin texture has recently attracted great attentions due to its potential application in future spintronic devices [3-10]. It is stable against moderate perturbation and has been observed in a variety of magnetic systems with the Dzyaloshinskii-Moriya (DM) interaction [3-4,11-18]. In particular, skyrmion can be easily driven to move by charge and spin currents [7,19-23], electric fields [24], heat flows [25-28], and microwaves [29-30]. Under the framework of the Thiele's equation [7,22-23,31-33], skyrmions are described by classical dynamical theory of a quasi-particle with intrinsic quantities such as mass and charge [34]. However, the moment of inertia of the skyrmion has never been discussed. Recent experimental observation of skyrmions in nanodisks provides an ideal platform to study the skyrmion's moment of inertia. The confinement from the disk boundary and interaction between skyrmions completely freezes the motion along the radial direction [14,28,35]. Unlike the free motion of skyrmions in bulks or two-dimensional films, multi-skyrmions in the nanodisks can only rotate in the tangential direction under any external perturbative magnetic field [28].

In the present work, we perform a theoretical study on the motion of multi-skyrmion cluster states in a small nanodisk. We find that an in-plane magnetic field determines the equilibrium orientation of

the cluster, whose oscillation around the equilibrium position behaves similarly as a rotating torsion pendulum about a perpendicular axis. The moment of inertia of skyrmions is derived both analytically and numerically. As a forced torsion pendulum, the multi-skyrmion cluster can be forced to rotate uniformly by rotating the magnetic field in the plane.

## Micromagnetic simulations

The static and dynamic states of the multi-skyrmion cluster in a nanodisk are studied using micromagnetic simulation with the OOMMF code including the DM interaction [36]. The DM interaction is assumed to be bulk origin with the energy density $e_{\mathrm{DM}} = D\mathbf{m}\cdot(\nabla\times\mathbf{m})$, where $D$ is the DM interaction constant, and $\mathbf{m}$ is the unit vector representing the orientation of the magnetization. A 5 nm-thick nanodisk with radius $R$ is under investigation, which is divided into discrete cells with size of $2\times2\times5\ \mathrm{nm}^3$. The material parameters used for the simulations correspond to the values in bulk FeGe [37]: the saturation magnetization $M_s = 3.84\times10^5\ \mathrm{A/m}$, the exchange constant $A = 8.78\times10^{-12}\ \mathrm{J/m}$, the DM interaction constant $D = 1.58\times10^{-3}\ \mathrm{J/m}^2$, and the Gilbert damping constant $\alpha = 0.01$.

Calculation of the dynamic response of multi-skyrmion cluster in our simulation involves two steps. The first step is the creation of the multi-skymion state in the disk. To this end, the nanodisk is cooled down gradually from 340K to zero temperature. The thermal fluctuation is introduced by including an additional stochastic field $\mathbf{h}_{th}(\mathbf{r},t)$ into the effective field. The average of the thermal field is averaged out, $\langle\mathbf{h}_{th}(\mathbf{r},t)\rangle = 0$, and satisfies the fluctuation-dissipation theorem $\langle\mathbf{h}_{th,i}(\mathbf{r},t)\mathbf{h}_{th,j}(\mathbf{r}',t')\rangle = 2\alpha k_B T/(\mu_0\gamma M_s\Delta V\Delta t)\delta_{i,j}\delta(\mathbf{r}'-\mathbf{r})\delta(t'-t)$, where $i,j = x,y,z$, $k_B$ is the Boltzmann constant, $T$ is the temperature, $\gamma$ is the gyromagnetic ratio, $\Delta V$ is volume of the cell, and $\Delta t$ is the simulation time step. During the cooling process, a perpendicular magnetic field is

used to adjust the number of skyrmions in the disk. Supplementary Videos 1-4 show the formation of multi-skyrmions with different numbers when the nanodisk is cooled down under different perpendicular fields [38]. After cooling, taking the state at zero temperature as the initial state and relaxing it under different perpendicular fields $H_z$, the skyrmion number will not change. In this way, we can successfully obtain the multi-skyrmion states under different $H_z$'s. A typical magnetic configuration of two-skyrmion cluster is shown in Fig. 1(a). The magnetic moment at the skyrmion core is pointing along -*z* direction, while the peripheral moments are pointing along +*z*. At the disk edge, the magnetization tilts slightly towards the disk plane due to the unbalanced DM interaction [39-40].

## Results and Discussions

We first turn to investigate the effect of a weak in-plane magnetic field on the equilibrium positions of two-skyrmion cluster state. To do so, we mark one skyrmion as S1, and use the axis linking the center to S1 as the referenced axis, as shown in Figure 1(a). After applying an in-plane magnetic field, fixed along *x*-axis, the skyrmion cluster rotates as a rigid body, as no change of their morphology and separation has been observed. After sufficiently long relaxation time, the cluster oscillates around an equilibrium direction, and eventually the reference axis stays parallel with the in-plane field along *x*-direction. This phenomenon indicates that the in-plane field determines a particular direction energetically favored. Deviation from these directions increases the energy of the system, which was further confirmed by comparing the system energy at varied angle $\phi_{S1}$ between the reference axis and *x* axis, as shown in Fig. 1(b), where $\delta E(\phi_{S1}) = E(H_x, \phi_{S1}) - E(0, \phi_{S1})$ with $E(H_x, \phi_{S1})$ and $E(0, \phi_{S1})$ the energies of system after and before $H_x$ is applied, respectively. As expected, $\delta E$ achieves the maximum for $\phi_{S1} = \pi/2$ or $3\pi/2$, but reaches the minimal for $\phi_{S1} = 0$

or $\pi$. It indicates that alignment between the reference axis and in-plane magnetic field gives rise to the energy minimum indeed. We also studied the relation between the angle of preferred direction $\phi_e$ and that of the in-plane magnetic field $\phi_H$, both measured from the *x*-axis. Figure 1(c) shows the variation of the angle $\phi_e$ with $\phi_H$ changing from $-\pi/2$ to $3\pi/2$. It obeys $\phi_e = \phi_H$ with a period of $\pi$. This confirms that the reference axis that linking the center of the two skyrmions always rotates to the direction of the applied field.

The magnetization dynamics of how the two-skyrmion cluster relaxes to the preferred direction is investigated in more detail. Fig. 2(a) shows the time (*t*) dependence of the angle $\phi_{S1}$ when the field $H_x$ is applied along the *x*-axis. Typical snapshots taken at different times after the application of $H_x$ are presented in Fig. 2(b) (see also Supplementary Video 5 [41]). A damped oscillation about the *x*-axis is clearly observed. It fits well to the usual oscillation formula $\phi_{S1}(t) = \phi_A e^{-\beta t}\cos(\omega t + \pi)$, where the maximum amplitude of the angle $\phi_A = 0.89$, the damping coefficient $\beta = 18$ MHz, and the frequency of the oscillation $\omega = 263$ MHz. The parameters that describe the damped oscillation for small rotation angles gives less difference from the results for the large rotation angles. The inset in Fig. 2(a) shows the damped sine fit to the simulation data after 83 ns, where $\phi_{S1}$ is much smaller, the fitted paraneters are $\phi_A = 0.897$, $\beta = 18.9$ MHz, and $\beta = 267$ MHz, almost the same as the fitting result above. It implies that the oscillation of the two-skyrmions cluster driven by an in-plane magnetic field is equivalent to that of a torsional pendulum, and the skyrmion-skyrmion and the skyrmion-field interactions provide the restoring torque in the torsional pendulum analogy.

This damped oscillator behavior can be thoroughly understood from the Landau-Lifshitz-Gilbert equation (LLG)

$$\frac{d\mathbf{m}}{dt} = -\frac{\gamma}{M_s}\mathbf{m}\times\frac{\partial E}{\partial \mathbf{m}} + \alpha\mathbf{m}\times\frac{d\mathbf{m}}{dt}, \quad (1)$$

where $E$ is the energy. Using sphere coordination, the magnetization components are written as $\mathbf{m}_x = \sin\theta\cos\varphi, \mathbf{m}_y = \sin\theta\sin\varphi, \mathbf{m}_z = \cos\theta$, where $\theta$ and $\varphi$ are inclination and azimuthal angles of $\mathbf{m}$ respectively. The LLG equation can then be transformed into two coupled equations:

$$\begin{aligned} \sin\theta\frac{d\varphi}{dt} - \alpha\frac{d\theta}{dt} &= \frac{\gamma}{M_s}\frac{\partial E}{\partial\theta} \\ \frac{d\theta}{dt} + \alpha\sin\theta\frac{d\varphi}{dt} &= -\frac{\gamma}{M_s\sin\theta}\frac{\partial E}{\partial\varphi} \end{aligned} . \tag{2}$$

When the skyrmions rotate in the disk, $\mathbf{m}(r,\phi) = \mathbf{m}(r,\phi+\omega t)$, i.e. $\theta(r,\phi) = \theta(r,\phi+\omega t)$, $\varphi(r,\phi) = \varphi(r,\phi+\omega t)$, where $r,\phi$ are the cylindrical coordinate of the point in the disk, and $\omega$ is the rotating frequency. Thus, $d\theta/dt = (\boldsymbol{\omega}\times\mathbf{r})\cdot\nabla\theta$ and $d\varphi/dt = (\boldsymbol{\omega}\times\mathbf{r})\cdot\nabla\varphi$. Accordingly, Eq. (2) becomes

$$\mathbf{g}\times(\boldsymbol{\omega}\times\mathbf{r}) - \alpha d(\boldsymbol{\omega}\times\mathbf{r}) = \nabla E \tag{3}$$

where $\mathbf{g} = (M_s/\gamma)\sin\theta(\nabla\theta\times\nabla\varphi)\hat{z}$ and $d = (M_s/\gamma)[(\nabla\theta)^2 + \sin^2\theta(\nabla\varphi)^2]$. Let $\mathbf{r}\times$Eq. (3), we obtain $-\alpha d\mathbf{r}\times(\boldsymbol{\omega}\times\mathbf{r}) = \mathbf{r}\times\nabla E$, where $\mathbf{r}\times\nabla E = \partial E/\partial\theta\hat{z}$. For the whole disk, it has $-\int\alpha d\mathbf{r}\times(\boldsymbol{\omega}\times\mathbf{r})dV = \int\mathbf{r}\times\nabla E dV$. Since only variations corresponding to rotation are of interest, the right term is $\int\mathbf{r}\times\nabla E\,dV = \partial E_{tot}/\partial\phi_{S1}\hat{z}$. The equation for the whole disk is thus can be written as

$$-\int d\alpha\mathbf{r}\times(\omega\times\mathbf{r})dV = \frac{\partial E_{tot}}{\partial\phi_{S1}}\hat{z} \tag{4}$$

The term on the left of Eq. (4) corresponds to the damping torque, which is denoted by $M_D$. It is can be written as $M_D = -\int\alpha d\mathbf{r}\times(\boldsymbol{\omega}\times\mathbf{r})dV = D\mathbf{X}\times(\mathbf{X}\times\boldsymbol{\omega})$, where $D = \alpha M_s L/\gamma\int(\nabla\theta)^2 + \sin^2\theta(\nabla\varphi)^2 dxdy$ [33], $\mathbf{X} = (x, y)$ is the position vector of the skyrmions, and $L$ is the thickness of the nanodisk. Here $D$ is proportional to the Gilbert damping coefficient, which determines the times scale of the relaxation. To obtain the expression of $\partial E_{tot}/\partial\phi_{S1}$, we need to analyze the variation of the total energy induced by the in-plane magnetic field. Fig. 3 shows the relation between total energy and $\phi_s^2$ with $\phi_s = \phi_A e^{-\beta t}$. A rough linear relation between them is

obtained, $E_{tot} = \frac{1}{2} k \phi_s^2$, where the constant $k$ is the counterpart of the spring constant in torsional pendulums. According to the law of energy conservation, we have the total energy $E_{tot} = E_p + E_v$. Here, $E_p = \frac{1}{2} k \phi_{S1}{}^2$ is the potential energy. $E_v = \frac{1}{2} I_0 \omega^2$ is the kinetic energy of rotation, where $I_0$ is the moment of inertia of the skyrmions about the center of the disk, and $\omega = d\phi_{S1}/dt$ is the angular frequency. Substituting the $E_{tot}$ into the Eq. (4), we obtain the dynamics equation that describe the oscillation of two-skyrmion cluster as

$$I_0 \frac{d\omega}{dt} = \mathbf{M}_p + \mathbf{M}_D \quad , \tag{5}$$

where $\mathbf{M}_p = -dE_p/d\phi_{S1}$ is the restoring torque relative to the disk center acting on the skyrmion cluster generated by the potential energy. Finally, inserting $\mathbf{M}_p$ and $\mathbf{M}_D$ into Eq. (8), the equation of motion of the cluster rotation is given by

$$\frac{d^2\phi_{S1}}{dt^2} + 2\beta \frac{d\phi_{S1}}{dt} + \omega_0^2 \phi_{S1} = 0 \, , \tag{6}$$

where $\beta = D|\mathbf{X}|^2 / 2I_0$ with inverse of which is the relaxation time, and $\omega_0^2 = k/I_0$. The solution of Eq. (6) is $\phi_{S1}(t) = \phi_A e^{-\beta t} \cos(\omega t + \phi_0)$, where $\omega = \sqrt{\omega_0^2 - \beta^2}$, and $\phi_0$ is the initial phase. This theoretical result precisely describes the damped oscillation of the simulation data.

The above analysis shows that the in-plane magnetic field induces a parabolic potential around the preferred direction. Similar to elastic potential energy in the torsional pendulum, this potential energy generates a restoring torque relative to the disk center acting on the skyrmion cluster, which induces the damped oscillation of the multi-skyrmion cluster, and finally stabilizes them along the easy axis. The proposed physics behind the field-driven rotation is different from previous reports of the skyrmion rotation. The rotation of a skyrmion lattice in Ref. 17 is induced by breaking the symmetry by a thermal gradient, while in Ref. 42 it is driven by a field gradient. In our study, the

confining potential breaks translational symmetry explicitly, and eventually generates the oscillation.

In the damped oscillation, the damping factor $\beta$ directly relates to the intrinsic moment of inertia of skyrmions by

$$I_s = \frac{\alpha D |\mathbf{X}|^2}{2n\beta}. \quad (7)$$

By fitting the oscillation curves, we can obtain $\beta$ and $I_s$ in consequence. Figure 4(a) shows the fitted $\beta$ as a function of the in-plane fields. No dependence between them has been observed. On the other hand, figure 4(b) demonstrates the $H_z$-dependence of $\beta$ at various disk radius $R$, and the corresponding $I_s$ is contour plotted in Fig. 4(d). $I_s$ increases monotonically with the increased $H_z$ and $R$. For example, for 115-nm-radius disk the value of $I_s$ is $5.9\times10^{-38}$ $\mathrm{Kg\cdot m^2}$ at $H_z$ =500 mT, while it increases almost linearly to $2.1\times10^{-37}$ $\mathrm{Kg\cdot m^2}$ by expanding the radius to 150 nm. Likewise, the value of $I_s$ for the skyrmions in 115-nm-radius disk increases from $5.9\times10^{-38}$ to $2.3\times10^{-37}$ $\mathrm{Kg\cdot m^2}$ when $H_z$ increases from 500 to 700 mT. In general, the disk with larger $R$ at larger $H_z$ corresponds to a larger $I_s$, it reaches $12.9\times10^{-37}$ $\mathrm{Kg\cdot m^2}$ for 150-nm-radius disk at $H_z$ =700 mT.

The existence of moment of inertia of skyrmions also gives rise to the inertia behavior when the in-plane magnetic field is turned off. As a result, the dynamics of skyrmions depends on the initial velocity of the skyrmions. To further confirm the existence of moment of inertia of skyrmions, the in-plane magnetic field is turned off at two typical times. One selected time is $t_A$ (Fig. 2(a)), at which the velocities of the skyrmions are zero. In this case, the simulation shows that these two skyrmions do not move anymore and stay where they are after turning off the magnetic field. But, if the in-plane magnetic field is turned off at another time $t_B$ (Fig. 2(a)), the two skyrmions continue to rotate, get

de-accelerated though. As shown in Fig. 5, the simulated angle $\phi_{S1}$ obeys the expected formula $\phi_{S1}(t) = (-\omega_{t_B}/2\beta)e^{-2\beta t} + (\phi_{t_B} + \omega_{t_B}/2\beta)$ (red line) obtained from the Eq. (6) by assuming $k$=0, where $\phi_{t_B}$ and $\omega_{t_B}$ are the value of $\phi_{S1}$ and angular frequency of the skyrmion at time $t_B$.

Overall results have confirmed the existence of moment of inertia and the damped nature of the skyrmion oscillation. Therefore, it is expected that the two skyrmions will be forced to rotate when an oscillated in-plane field is applied. The field can be written as: magnetic field $\mathbf{H} = H_0(\cos(\omega_H t + \varphi_H)\hat{\mathbf{i}} + \sin(\omega_H t + \varphi_H)\hat{\mathbf{j}})$, the oscillation of skyrmions then obeys the equation of motion

$$\frac{d^2\phi_{S1}}{dt^2} + 2\beta\frac{d\phi_{S1}}{dt} + \omega_0^2\phi_{S1} - \omega_0^2(\omega_H t + \varphi_H) = 0. \tag{8}$$

Its solution is

$$\phi_{S1}(t) = \phi_A e^{-\beta t}\cos\omega t + (\omega_H t + \varphi'). \tag{9}$$

where $\varphi'$ is phase. The angular frequency is

$$\omega_r = \frac{d\phi_{S1}}{dt} = \phi_A e^{-\beta t}(-\beta\cos(\omega t) - \omega\sin(\omega t)) + \omega_H. \tag{10}$$

To verify this prediction, the corresponding micromagnetic simulations have been performed. Considering the oscillation frequency of skyrmions that ranges from dozens to hundreds of MHz, the field is designed to have the same frequency range because too high frequency can be hardly responded by skyrmions. As a typical illustration, Fig. 6(a) shows the time evolution of the angle $\phi_{S1}$ and the corresponding angular frequency $\omega_r$ when a field with $\omega_H = 126$ MHz and $\varphi_H = \pi/4$ is applied. The simulation results (the circles) are perfectly fitted to the theory (the lines). At $t \to \infty$, $\phi_{S1}(t) \to \omega_H t + \varphi'$, and the angular frequency $\omega_r$ converges to $\omega_H$, which means that a uniform rotation can be achieved by applying a rotating magnetic field. The trajectories of the two

skyrmions shown in Fig. 6(b) confirm the uniform rotation. The whole simulation movie is provided in Supplementary Video 6 [43].

So far we have discussed the rotation and moment of inertia of two-skyrmion. Similar damped oscillation and forced rotation are also observed in multi-skyrmion clusters. Figure 7 shows the relaxation of multi-skyrmion clusters under a constant field applied along *x*-direction. Number of skyrmions *n* varies from 3 to 5. To minimize the skyrmion-skyrmion and skyrmion-edge interactions, skyrmions self-assemble into high-symmetry configurations, such as equilateral triangle, square, and pentagon, depending on the number of skyrmions. Obviously, after applying an in-plane magnetic field along *x*-axis, the skyrmion clusters again rotate as rigid bodies without change of their morphology and relative separations. Simulations of the detailed magnetization dynamics also indicates that this rotation is achieved by the damped oscillation like the case of two skyrmions.

Uniform rotations induced by rotating magnetic field also persist for multi-skyrmion clusters. Figure 8 shows the uniform rotation frequency when a rotating magnetic field with $\omega_H = 12.56\ \mathrm{MHz}$ is applied. Let $n_l$ be the number of the sides of the polyhedron formed by skyrmions. The rotation frequencies obey the quantization rule $|\omega_r| = \omega_H / n_l$ when is $n_l$ odd, while $|\omega_r| = \omega_H$ when $n_l$ is even. Notice that the presence of a central skyrmion does not change the value of $n_l$. Interestingly, under a counter clockwise rotating field, skyrmions rotate clockwise for $n_l = 3$ and 7, but rotate counter clockwise for $n_l = 2$, 4, 5 and 6. The effect of anisotropy brought by the lattice has been ruled out by changing for different mesh sizes and different mesh shapes. Indeed, both rotation frequency and rotation direction have no dependence on other factors, such as the size of the nanodisk, in-plane rotating magnetic field, and the perpendicular field $H_z$.

## Conclusion

In conclusion, we have demonstrated that rotation of the multi-skyrmion cluster confined in a nanodisk can be driven by an in-plane magnetic field. The rotation is accompanied by a damped oscillation of the skyrmions around the energy minima due to the presence of moment of inertia. Taking advantage of the relation between multi-skyrmions and in-plane magnetic fields, we can excite the uniform rotation of multi-skyrmion cluster by a rotating in-plane magnetic field. The rotation frequencies are quantized by the number of skyrmions therein. Our study not only provides a new mechanism to control multi-skyrmions states in confined geometries, but also assigns skyrmion clusters a new intrinsic entity, the moment of inertia. More recently, we have directly observed the multi-skyrmion cluster states in FeGe nanodisk by using Lorentz Transmission Electron Microscope (TEM) [44]. Our prediction can thus be observed in this system.

## Acknowledgments

This work was supported by the National Natural Science Foundation of China (Grant No. 11404053). Work at UNH was supported by the U.S. Department of Energy (DOE), Office of Science, Basic Energy Sciences (BES) under Award No. DE-SC0016424.

## APPENDIX: INFLUENCE OF THE DISCRETED GRID

One thing must be noted is that the preferred direction exists even in absence of the in-plane magnetic field, which is induced by the discrete square grid on the disk in the simulation. Figure 9 shows the variation of total energy of the nanodisk with the angle of skyrmion S1 $\phi_{S1}$. Because the angular symmetry is commensurate with the square grid, the energy difference caused by the square grid is most obvious for four-skyrmions state. The total energy achieves the maximum for $\phi_{S1} = 0$ and $\pi/2$, while it reaches the minimal for $\phi_{S1} = \pi/4$ and $3\pi/4$. The energy difference is

$5.4\times10^{-22}$ J. It needs at least 90-mT-strength in-plane magnetic field to overcome this energy barrier to drag the skyrmion S1 from $\phi_{S1}=0$ to $\phi_{S1}=\pi/4$. This square-grid-induced energy difference exists for two skyrmions as well. However, the total energy achieves minima at $\phi_{S1}=\pi/4$ and $3\pi/4$, and the energy difference is reduced to $1.9\times10^{-22}$ J. The minimal in-plane magnetic field to drag S1 from the directions of $\phi=\pi/4$ to *x*-axis is about 8 mT. For three- and five-skyrmions states, this energy difference does not exist because the three- and five-fold rotational symmetries are incommensurate with the square grid.

## References


[1] E. Saitoh, H. Miyajima, T. Yamaoka, and G. Tatara, Nature **432**, 203 (2004).

[2] J. Rhensius, L. Heyne, D. Backes, S. Krzyk, L. J. Heyderman, L. Joly, F. Nolting, and M. Kläui, Phys. Rev. Lett. **104**, 067201 (2010).

[3] S. Mühlbauer, B. Binz, F. Jonietz, C. Pfleiderer, A. Rosch, A. Neubauer, R. Georgii, and P. Böni, Science **323**, 915 (2009).

[4] X. Z. Yu, Y. Onose, N. Kanazawa, J. H. Park, J. H. Han, Y. Matsui, N. Nagaosa, and Y. Tokura, Nature **465**, 901 (2010).

[5] N. Nagaosa and Y. Tokura, Nat. Nanotechnol. **8**, 899 (2013).

[6] N. Romming, C. Hanneken, M. Menzel, J. E. Bickel, B. Wolter, K. von Bergmann, A. Kubetzka, and R. Wiesendanger, Science **341**, 636 (2013).

[7] R. Tomasello, E. Martinez, R. Zivieri, L. Torres, M. Carpentieri, and G. Finocchio, Sci. Rep. **4**, 6784 (2014).

[8] Y. Liu, H. F. Du, M. Jia, and A. Du, Phys. Rev. B **91**, 094425 (2015).

[9] Y. Zhou and M. Ezawa, Nat. Commun. **5**, 4652 (2014).

[10] Y. Zhou, E. Iacocca, A. A. Awad, R. K. Dumas, F. C. Zhang, H. B. Braun, and J. Äkerman, Nat. Commun. **6**, 8193 (2015).

[11] X. Z. Yu, N. Kanazawa, Y. Onose, K. Kimoto, W. Z. Zhang, S. Ishiwata, Y. Matsui, and Y. Tokura, Nat. Mater. **10**, 106 (2011).

[12] S. Heinze, K. von Bergmann, M. Menzel, J. Brede, A. Kubetzka, R. Wiesendanger, G. Bihlmayer, and S. Blügel, Nat. Phys. **7**, 713 (2011).

[13] S. Seki, X. Z. Yu, S. Ishiwata, and Y. Tokura, Science **336**, 198 (2012).

[14] H. F. Du, W. Ning, M. L. Tian, and Y. H. Zhang, Phys. Rev. B **87**, 014401 (2013).

[15] M. Nagao, Y.-G. So, H. Yoshida, M. Isobe, T. Hara, K. Ishizuka, and K. Kimoto, Nat. Nanotechnol. **8**, 325 (2013).

[16] K. Shibata, X. Z. Yu, T. Hara, D. Morikawa, N. Kanazawa, K. Kimoto, S. Ishiwata, Y. Matsui, and Y. Tokura, Nat. Nanotechnol. **8**, 723 (2013).

[17] Y. Tokunaga, X.Z. Yu, J.S. White, H.M. Røn now, D. Morikawa, Y. Taguchi, and Y. Tokura, Nat. Commun. **6**, 7638 (2015).

[18] W. Jiang, P. Upadhyaya, W. Zhang, G. Yu, M. B. Jungfleisch, F. Y. Fradin, J. E. Pearson, Y. Tserkovnyak, K. L. Wang, O. Heinonen, S. G. E. te Velthuis, and A. Hoffmann, Science **349**, 283 (2015).

[19] F. Jonietz, S. Mühlbauer, C. Pfleiderer, A. Neubauer, W. Münzer, A. Bauer, T. Adams, R. Georgii, P. Böni, R. A. Duine, K. Everschor, M. Garst, and A. Rosch, Science **330**, 1648 (2010).

[20] J. Zang, M. Mostovoy, J. H. Han, and N. Nagaosa, Phys. Rev. Lett. **107**, 136804 (2011).

[21] X. Z. Yu, N. Kanazawa, W. Z. Zhang, T. Nagai, T. Hara, K. Kimoto, Y. Matsui, Y. Onose, and Y. Tokura, Nat. Commun. **3**, 988 (2012).

[22] J. Iwasaki, M. Mochizuki, and N. Nagaosa, Nat. Commun. **4**, 1463 (2013).

[23] S. F. Zhang, J. B. Wang, Q. Zheng, Q. Y. Zhu, X. Y. Liu, S. J. Chen, C. D. Jin, Q. F. Liu, C. L. Jia, and D. S. Xue, New J. Phys **17**, 023061 (2015).

[24] J. S. White, K. Prša, P. Huang, A. A. Omran, I. Živković, M. Bartkowiak, H. Berger, A. Magrez, J. L. Gavilano, G. Nagy, J. Zang, and H. M. Rønnow, Phys. Rev. Lett. **113**, 107203 (2014).

[25] L.Y. Kong and J. D. Zang, Phys. Rev. Lett. **111**, 067203 (2013).

[26] R. E. Troncoso and A. S. Núñez, Phys. Rev. B **89**, 224403 (2014).

[27] S.-Z. Lin, C. D. Batista, C. Reichhardt, and A. Saxena, Phys. Rev. Lett. **112**, 187203 (2014).

[28] M. Mochizuki, X. Z. Yu, S. Seki, N. Kanazawa, W. Koshibae, J. Zang, M. Mostovoy, Y. Tokura, and N. Nagaosa, Nat. Mater. **13**, 241 (2014).

[29] Y. Y. Dai, H. Wang, T. Yang, W. J. Ren, and Z. D. Zhang, Sci. Rep. **4**, 6153 (2014).

[30] W. Wang, M. Beg, B. Zhang, W. Kuch, and Hans Fangohr, Phys. Rev. B **92**, 020403 (2015).

[31] J. Iwasaki, M. Mochizuki, and N. Nagaosa, Nat. Nanotechnol. **8**, 742 (2013).

[32] J. Sampaio, V. Cros, S. Rohart, A. Thiaville, and A. Fert, Nat. Nanotechnol. **8**, 839 (2013).

[33] A. A. Thiele, Phys. Rev. Lett. **30**, 230 (1973).

[34] F. Büttner, C. Moutafis, M. Schneider, B. Krüger, C. M. Günther, J. Geilhufe, C. v. K. Schmising, J. Mohanty, B. Pfau, S. Schaffert, A. Bisig, M. Foerster, T. Schulz, C. A. F. Vaz, J. H. Franken, H. J. M. Swagten, M. Kläui, and S. Eisebitt, Nat. Phys. **11**, 225 (2015). C. Schütte, J. Iwasaki, A. Rosch, and N. Nagaosa, Phys. Rev. B **90**, 174434 (2014).

[35] Y. Shimada and J. Ohe, Phys. Rev. B **91**, 174437 (2015).

[36] We used the 1.2a5 version of the OOMMF code. See http://math.nist.gov/oommf.

[37] M. Beg, R. Carey, W. Wang, D. Cortés-Ortuño1, M. Vousden, M. Bisotti, M. Albert, D. Chernyshenko, O. Hovorka, R. L. Stamps, and H. Fangohr, Sci. Rep. **5**, 17137 (2015).

[38] See Supplemental Material at URL for the formation of two skyrmions in the nanodisk under a 550 mT perpendicular cooling field, URL for the formation of three skyrmions in the nanodisk under a 510mT perpendicular cooling field, URL for the formation of four skyrmions in the nanodisk under a 500 mT perpendicular cooling field, URL for the formation of five skyrmions in the nanodisk under a 450 mT perpendicular cooling field.

[39] H. F. Du, W. Ning, M. L. Tian, and Y. H. Zhang, EPL, **101**, 37001 (2013).

[40] S. Rohart and A. Thiaville, Phys. Rev. B **88**, 184422 (2013).

[41] See Supplemental Material at URL for the damped oscillation of two skyrmions driven by an in-plane magnetic field.

[42] K. Everschor, M. Garst, B. Binz, F. Jonietz, S. Muhlbauer, C. Pfleiderer, and A. Rosch, Phys. Rev. B **86**, 054432 (2012).

[43] See Supplemental Material at URL for the rotation of two skyrmions driven by a rotating magnetic field.

[44] X. Zhao, C. Jin, C. Wang, H. Du, J. Zang, M. Tian, R. Che, and Y. Zhang, PNAS **113**, 4918 (2016).

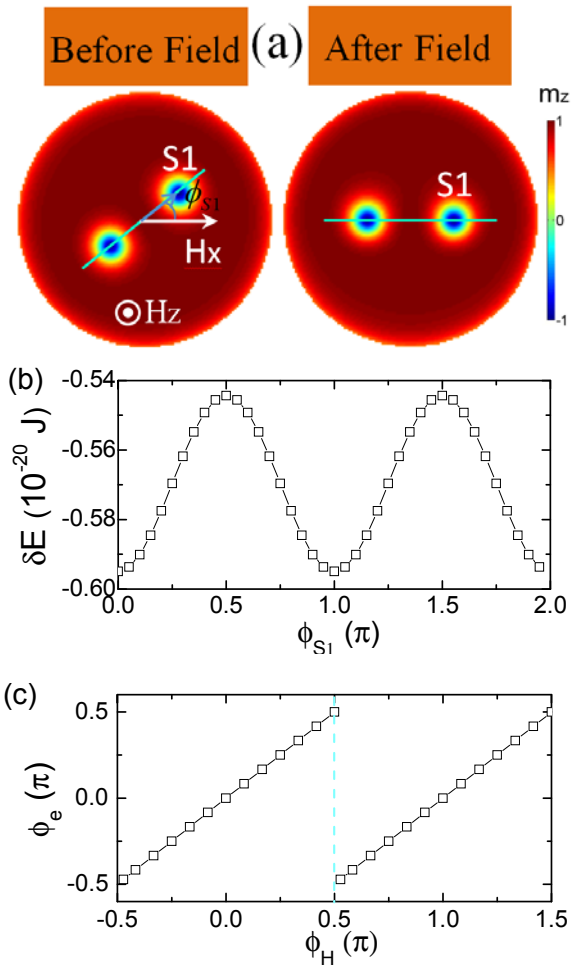


Figure 1 (a) Rotation of two-skyrmion cluster under an in-plane magnetic field along *x*-axis with $H_x$=15 mT, where the $m_z$ distribution in the nanodisk is plotted by color contour. $\phi_{S1}$ is the angle between the representative skyrmion S1 and *x*-axis. (b) The change in system energy $\delta E$ induced by $H_x$ as a function of $\phi_{S1}$. (c) The variation of $\phi_e$ , the preferred direction, as a function of $\phi_H$, the direction of the in-plane magnetic field.

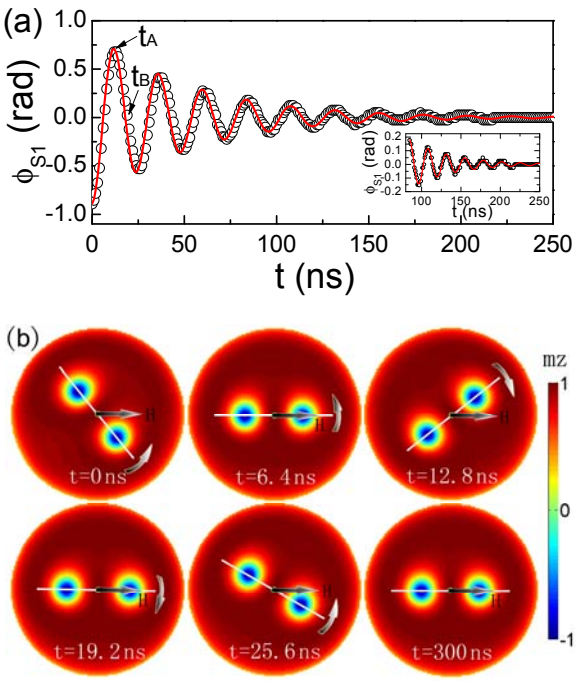


Figure 2 Damped oscillation of two skyrmions driven by an in-plane magnetic field. (a) Time evolution of $\phi_{S1}$ after the in-plane magnetic field is applied ($R$=115 nm, $H_x$=20 mT, and $H_z$=500 mT). The red curve is a damped sine fit to the simulation data. The inset shows the damped sine fit to the simulation data after 83 ns. (b) Snapshots of $m_z$ in the disk at different time after the application of the in-plane magnetic field.

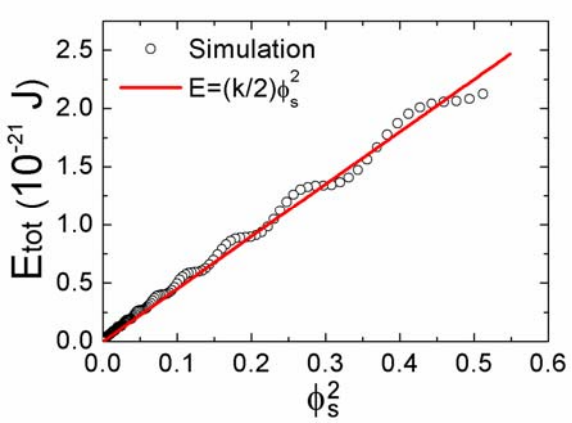


Figure 3 Total energy as a function of $\phi_s^2$ ($H_x$=20 mT, $R$=115 nm, $H_z$=500 mT), where $\phi_s = \phi_A e^{-\beta t}$.

The circle dots are the simulation data, and the red curve is the analytical result.

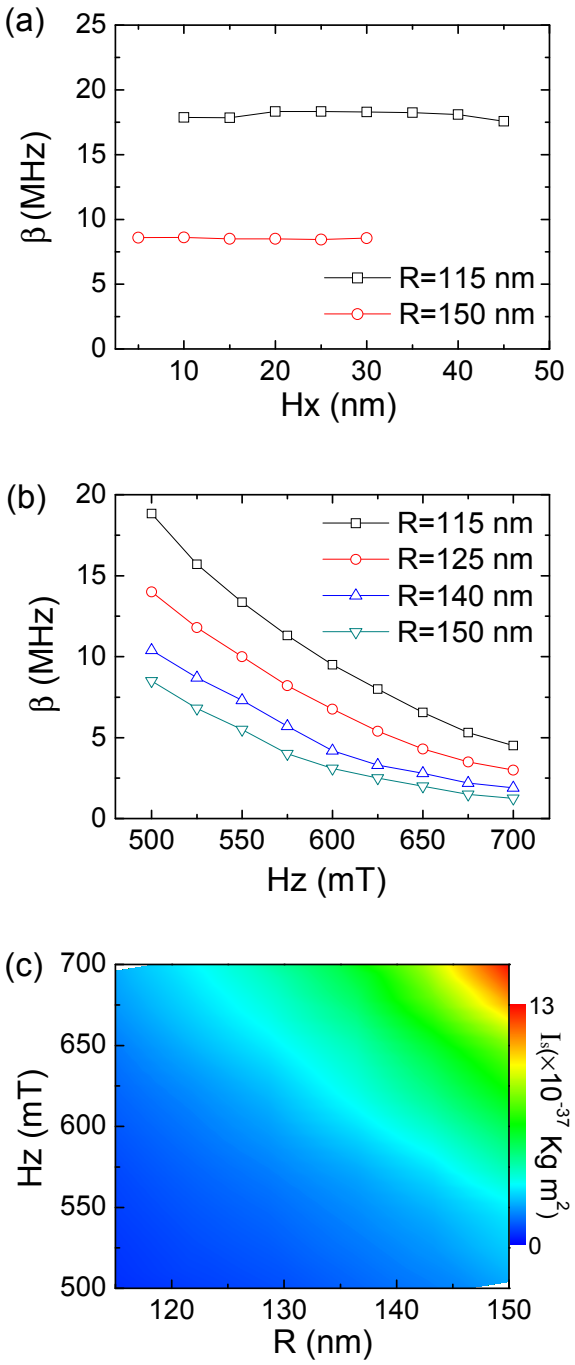


Figure 4 (a) The damping coefficient of amplitude ( $\beta$ ) as a function of $H_x$ for two skyrmions with $H_z$ =500 mT. (b) The fitted $\beta$ as a function of $H_z$ for two skyrmions in nanodisks with different radius. (c) Contour plot of $I_s$ versus disk radius $R$ and perpendicular magnetic field $H_z$.

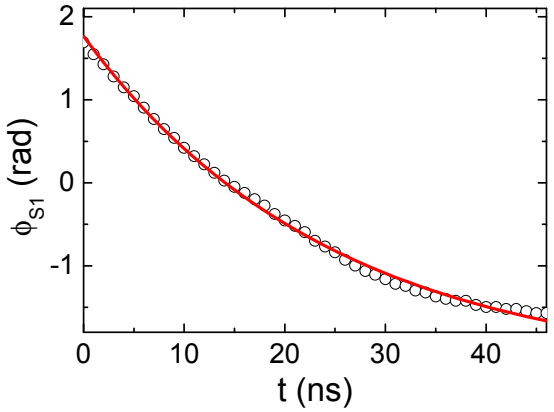


Figure 5 Time evolution of $\phi_{S1}$ after $H_x$ switched off at time $t_B$. The red curve is the analytical fit of the simulation data.

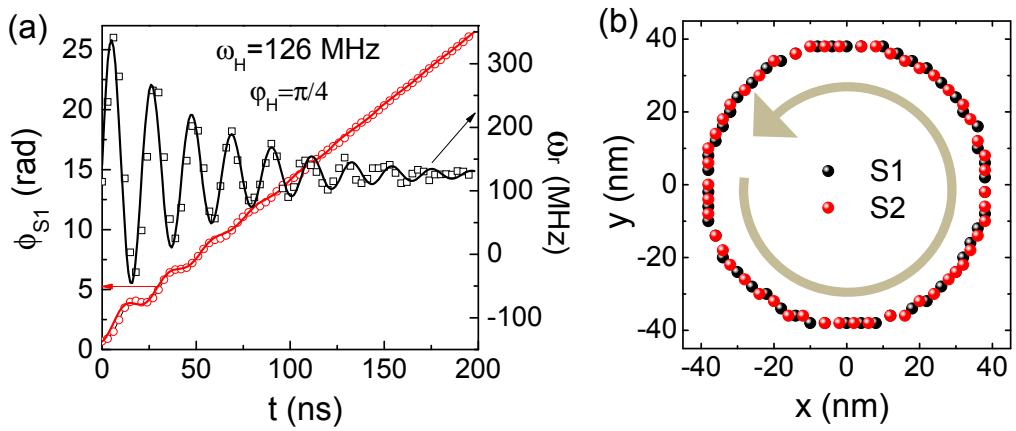


Figure 6 Forced rotation of two skyrmions by a rotating magnetic field in a disk with radius of 115 nm. (a) Time evolution of $\phi_{S1}$ and $\omega_r$ after the rotating magnetic field applied, where $H_0$=20 mT. The square and circle dots are the simulated data. The black and red curves correspond to the results obtained from the explicit expression of Eqs. (9) and (10), respectively. (b) The trajectories of the two skyrmions after 150 ns. The arrow indicates the rotation direction.

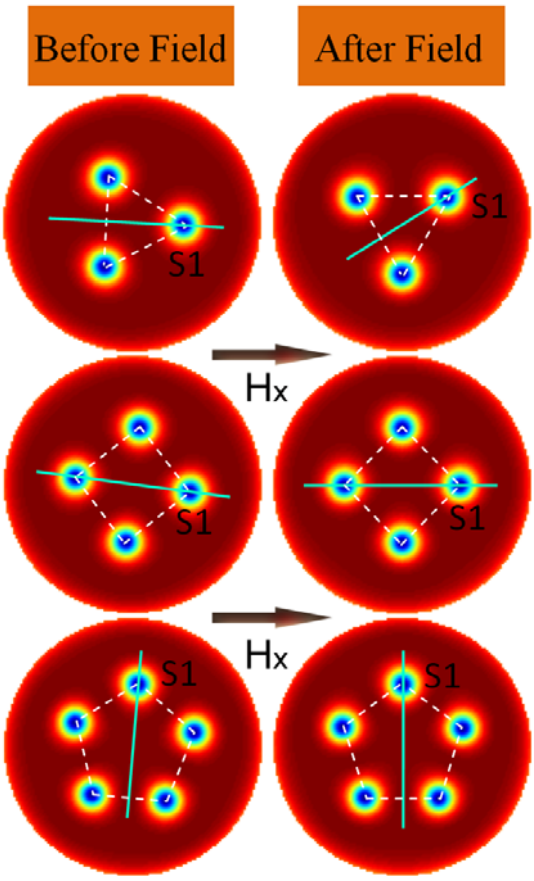


Figure 7 Rotations of multi-skyrmion clusters under an in-plane magnetic field along *x*-axis in nanodisks containing three, four and five skyrmions, respectively.

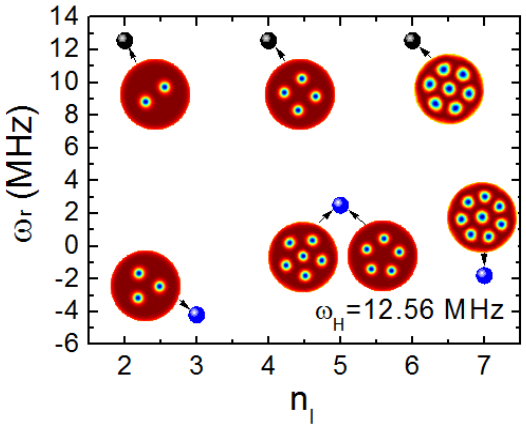


Figure 8 The steady rotation frequency of the skyrmions with different $n_l$ driven by a counter clockwise rotating magnetic field with frequency of 12.56 MHz, where the corresponding images of $m_z$ are shown.

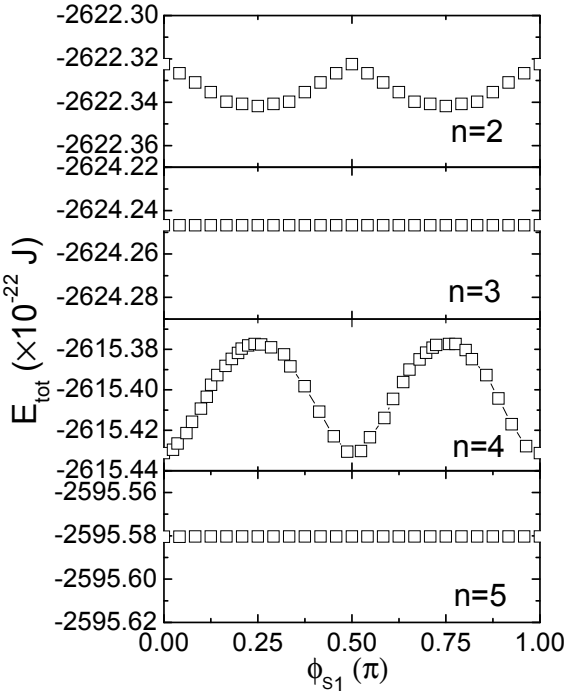


Figure 9 The total energy of the system as a function of $\phi_{S1}$ for multi-skyrmions cluster with different numbers.